SCIENCE CHINA
Chemistry

• ARTICLES •

September 2012 Vol.55 No.9: 1819–1824
doi: 10.1007/s11426-012-4731-6

A comparative study of the electrooxidation of C1 to C3 aliphatic alcohols on Ni modified graphite electrode

JAFARIAN M.[1], MIRZAPOOR A.[1], DANAEE I.[2*], SHAHNAZI Sangachin A. A.[2] & GOBAL F.[3]

[1]*Departement of Chemistry, K. N. Toosi University of Technology, Tehran, Iran*
[2]*Abadan Faculty of Petroleum Engineering, Petroleum University of Technology, Abadan, Iran*
[3]*Departement of Chemistry, Sharif University of Technology, Tehran, Iran*

Received April 4, 2011; accepted December 19, 2011; published online August 9, 2012

Nickel modified graphite electrodes (G/Ni) prepared by galvanostatic deposition were examined for their redox process and electrocatalytic activities towards the oxidation of methanol, ethanol, 1-propanol and 2-propanol in alkaline solutions. The methods of cyclic voltammetry (CV), chronoamperometry (CA) and impedance spectroscopy (EIS) were employed. In CV studies, the electrochemical response, peak current varied in the order of MeOH > EtOH > 1-PrOH > 2-PrOH. Under the CA regime, a higher catalytic rate constant obtained for methanol oxidation was in agreement with CV measurements. Lower charge transfer resistance was obtained for low carbon alcohols oxidation and significantly higher exchange current density was obtained for methanol oxidation.

alcohols, electrocatalytic, nickel, modified electrode, equivalent circuit

---

1 Introduction

Because of energy crisis and environmental affinity, fuel cells (FCs) are widely investigated and considered as one of the most important power recourses. Among several alcohols such as methanol, ethanol and propanol [1], which can be used in direct alcohol fuel cells (DAFCs), ethanol is the most promising one due to considerable energy density (≈ 8 kWh/kg), nontoxicity, biological renewability, easy handling and storage [2, 3]. It has been reported that ethanol is oxidized to acetaldehyde and CO_2 by a dual-path mechanism in which the oxidation to acetaldehyde and CO_2 proceeds through the dehydrogenation of adsorbed ethanol and adsorbed intermediates, respectively [4]. However, its oxidation is much more complex than methanol in view of the need to break the C-C bond to achieve total oxidation.

Methanol, which is generally considered as the most appropriate fuel for DAFCs [5] in spite of its toxicity and environmental problems because of high miscibility with water, has several offsetting advantages such as high efficiency, very low polluting emissions and potential renewability in addition to fast and convenient refueling [6, 7]. Methanol can undergo electrooxidation to formaldehyde, formic acid and CO_2 [5].

The electrooxidation of 2-propanol is known to start at much more negative potentials than that of methanol, while there has been relatively little research regarding the 2-propanol electrooxidation [8, 9]. 1-propanol and 2-propanol have different oxidation mechanisms; 1-propanol produces propanal, propionic acid, and CO_2, whereas 2-propanol produces acetone and CO_2. 2-propanol does not produce CO as a reaction intermediate because of the difficulties in carbon chain breaking due to the central positioning of the OH bond in 2-propanol. The absence of CO adsorption during the 2-propanol oxidation leads to a lower oxidation onset potential than that in methanol, ethanol, and 1-propanol [8]. As such, 2-propanol is a prospective fuel for

---

*Corresponding author (email: danaee@put.ac.ir)

DAFCs, as has been suggested in other studies [10, 11]. However, its reaction mechanism has not been fully described [11, 12, 13].

From a kinetic point of view, the anodic reaction is sluggish at moderate operating temperatures of the PEM type fuel cells because complex reaction steps are involved during the complete oxidation reaction; for instance, multi-electron transfers proceed together with consecutive adsorption/surface reactions/desorption of several reaction products and byproducts. In addition, some poisonous species (e.g., CO), which are produced during the electrooxidation of alcohols, are irreversibly adsorbed on the active surface sites of the Pt-based catalysts, thereby impeding the electrocatalysis. Even the complete oxidation of the simplest of alcohols (MeOH) involves six electrons pointing to the multi-steps nature of the process with several products or reaction intermediates.

Electrocatalytic oxidation of alcohols over various catalysts, which are mainly based on platinum, is the subject of a great number of studies [14]. Pt is one of the best anodic materials that exhibit catalytic properties for the oxidation process of alcohols to proceed at a sufficient rate in fuel cells [15], but the high cost of Pt makes it not economic for industrial applications. Consequently some research activities have been conducted to find new and less expensive materials as anodes for DAFCs [16].

Carbon is a common choice for supporting nanosized electrocatalyst particles in DAFCs because of its large surface area, high electrical conductivity, and pore structures [17–20]. However, this inert material (carbon) does not help electrocatalytic activities, but serves only as a mechanical support. A few studies have been reported in this regard, mostly using oxide materials as active or promoting supports [21, 22].

It is well established that nickel can be used as a catalyst due to its surface oxidation properties [23–26]. One of the very important uses of nickel as a catalyst is for the oxidation of alcohols. Ni produces very high anodic current but does not have suitable oxidation potential. Several studies of the electro-oxidation of alcohols on Ni and glassy carbon/Ni-oxides have been reported [27–29].

The purpose of the present work is to compare the electrochemical oxidation of methanol, ethanol, 1-propanol and 2-propanol on a nickel modified graphite electrode in a solution of 1 M NaOH in order to investigate the potential usefulness of higher alcohols as fuels in DAFCs.

2 Materials and methods

Sodium hydroxide, nickel sulfate, sodium citrate, ammonium sulfate and alcohols used in this work were Merck product of analytical grade and were used without further purification. Doubly distilled water was used throughout. Electrochemical studies were carried out in a conventional three-electrode cell powered by an electrochemical system comprising of EG&G model 273 potentiostat/galvanostat and Solartron model 1255 frequency response analyzer. The system is run by a PC through M270 and M398 commercial software via a GPIB interface. A dual Ag/AgCl-saturated KCl, a Pt wire and a graphite (G) disk electrode were used as the reference, counter and working electrodes, respectively. All studies were carried out at 298 K. The G disk electrode was polished with 0.05 mm alumina powder on a polishing microcloth and rinsed thoroughly with doubly distilled water prior to modification.

Films of nickel were formed on the graphite surface by galvanostatic deposition from a solution composed of 0.22 M $NiSO_4.6H_2O$, 0.4 M $C_6H_5Na_3O_7.2H_2O$ and 0.22 M $(NH_4)_2SO_4$ for Ni deposition at the current density of 7 mA cm^{-2} for 300 s. The working electrode was placed in the middle of the electrolyte, which was stirred with magnetic stirrer during electrodeposition. Fitting of experimental impedance spectroscopy data to the proposed equivalent circuit was done by means of home written least squares software based on the Marquardt method for the optimization of functions and Macdonald weighting for the real and imaginary parts of the impedance [30].

3 Results and discussion

Figure 1 presents consecutive cyclic voltammograms (CV) of a G/Ni electrode after 50 cycles in 1 M NaOH solution recorded at a potential sweep rate of 100 mV s^{-1}. In the first sweep, a pair of redox peaks appeared at 445 and 350 mV vs. Ag/AgCl, which are assigned to Ni^{2+}/Ni^{3+} redox couple in alkaline media. In the subsequent cycles, the peaks shift cathodically and stabilize at 420 and 305 mV vs. Ag/AgCl, respectively. The entire behavior is in accord with the data reported previously in the literature concerning the formation and interconversion of α and ß-phases of $Ni(OH)_2$, its conversion to NiOOH and the enrichment of Ni^{3+} species on or just beneath the surface [31–35]. In the subsequent cycles, both the anodic and cathodic peaks shift negatively and stabilize pointing to higher energies (potential) required for nucleation of NiOOH in the first cycle. The enhanced base line current of the first cycle is associated with the oxidation of Ni to Ni^{2+}. The current grows with the number of potential scans indicating the progressive enrichment of the accessible electroactive species Ni^{2+} and Ni^{3+} on or near the surface.

Figure 2 shows cyclic voltammograms of G/Ni electrode in 1 M NaOH solution in the presence of 0.1 M methanol, ethanol, 1-propanol and 2-propanol at a potential sweep rate of 10 mV s^{-1}. The activity order of alcohol oxidation on G/Ni electrode is methanol > ethanol > 1-propanol > 2-propanol. It seems that longer carbon branch suppresses the adsorption of alcohols to the surface [36]. At G/Ni electrode, oxidation of alcohols appeared as a typical electro-

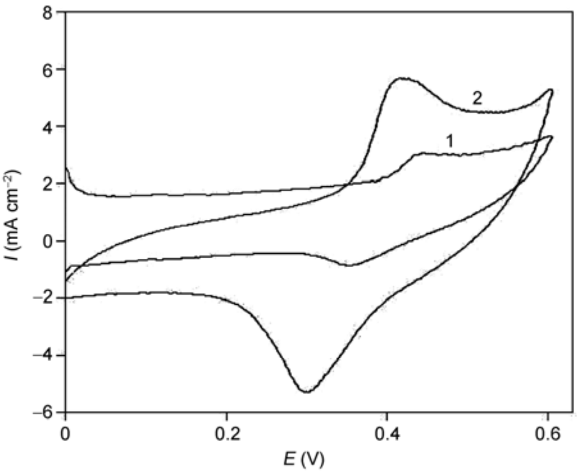

Figure 1 Consecutive cyclic voltammogram of G/Ni oxidation in 1 M NaOH composed of (1) first and (2) fiftieth cycle at a scan rate of 100 mV s^{-1}. The potential is against the Ag/AgCl reference electrode.

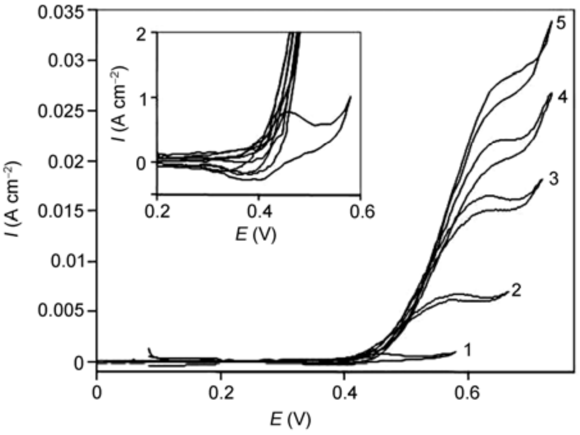

Figure 2 (a) Cyclic voltammograms in the absence (1) and presence of 0.1 M of (2) 2-propanol, (3) 1-propanol, (4) ethanol and (5) methanol on the G/Ni electrode in 1M NaOH solution. The potential sweep rate was 10 mV s^{-1}; (b) initial potential of alcohols oxidation. The potential is against the Ag/AgCl reference electrode.

catalytic response. The anodic current increased with respect to that observed for the modified surface in the absence of alcohols and it was followed by decreasing the cathodic current.

The decreased cathodic current that ensured the oxidation process in the reverse cycle indicates that the rate determining step certainly involves alcohols and that it is incapable of reducing the entire high valent nickel species formed in the oxidation cycle. The electrocatalytic oxidation of alcohols not only occurs in the anodic but also continues in the initial stage of the cathodic half cycle. Alcohol molecules adsorbed on the surface are oxidized at higher potentials parallel to the oxidation of Ni^{2+} to Ni^{3+} species. The latter process has the consequence of decreasing the number of sites for alcohols adsorption, which, along with the poisoning effect of the products or intermediates of the reaction, tends to decrease the overall rate of alcohols oxidation. Thus, the anodic current passes through a maximum as the potential is anodically swept. In the reverse half cycle, the oxidation continues and its corresponding current goes through the maximum due to the regeneration of active sites for adsorption of alcohols as a result of the removal of adsorbed intermediates and products. The rate of alcohols oxidation as signified by the anodic current in the cathodic half cycle drops as the unfavorable cathodic potentials are approached.

According to the high current density in the presence of alcohols and also observation of a new oxidation peak for alcohols oxidation at a potential much more positive than that of the oxidation of $Ni(OH)_2$ potential, we assume that part of the anodic current is due to alcohols oxidation by NiOOH due to the disappearance of the NiOOH reduction peak in the negative sweep, and part of the current is due to alcohols oxidation on the surface of the oxide layer by direct electro-oxidation [37, 38]. The redox transition of nickel species present in the film is

$$Ni^{2+} \rightleftarrows Ni^{3+} + e^{-} \tag{1}$$

and alcohol is oxidized on the modified surface via the following reaction

$$Ni^{3+} + \text{alcohol} \longrightarrow Ni^{2+} + \text{intermediate} \tag{2}$$

$$Ni^{3+} + \text{intermediate} \longrightarrow Ni^{2+} + \text{products} \tag{3}$$

$$Ni^{3+}\text{-alcohol} \longrightarrow Ni^{3+}\text{-intermediate} + e \tag{4}$$

$$Ni^{3+}\text{-intermediate} \longrightarrow Ni^{3+}\text{-products} + e \tag{5}$$

Observation of a high current density in the presence of alcohol in comparison to the $Ni(OH)_2$ is according to Eqs. (4) and (5).

Setting the working electrode potentials to desired values, we measured the catalytic rate constant of alcohol under chronoamperometric regime. Figure 3 shows double steps chronoamperograms for the G/Ni in the absence (1) and presence (2–6) of alcohols at the concentration of 0.1 M with an applied potential step of 650 and 300 mV, respectively. The current is negligible when the potential is stepped down to 300 mV, indicating the irreversibility of alcohols oxidation process. Chronoamperometry can also be used for evaluation of the catalytic rate constant according to [39]

$$\frac{I_{\text{cat}}}{I_{\text{L}}} = \gamma^{1/2}\left[\pi^{1/2} erf(\gamma^{1/2}) + \frac{\exp(-\gamma)}{\gamma^{1/2}}\right] \tag{6}$$

where I_{cat} and I_{L} are the currents of the G/Ni in the presence and absence of alcohols and $\gamma = kC^*t$ is the argument of the error function. k is the catalytic rate constant, C^* is bulk concentration of alcohols and t is elapsed time (s). In the cases where $\gamma > 1.5$, $erf(\gamma^{1/2})$ is almost equal to unity and the above equation simplifies to

$$\frac{I_{\text{cat}}}{I_{\text{L}}}=\gamma^{1/2}\pi^{1/2}=\pi^{1/2}(kC*t)^{1/2} \tag{7}$$

From the slope of the $I_{\text{cat}}/I_{\text{L}}$ vs. $t^{1/2}$ plot, presented in Figure 4, the mean value of k for methanol, ethanol, 1-propanol and 2-propanol at the concentration of 0.1 M was obtained as 3.1, 2.6, 1.4, and 0.93×10^3 $\text{cm}^3\,\text{mol}^{-1}\,\text{s}^{-1}$, respectively.

Figure 5(a) shows the Nyquist diagrams of G/Ni electrode recorded at the oxidation peak potential as dc-offset for 0.1 M selected low carbon alcohols. The Nyquist diagrams consisted of two slightly depressed overlapping capacitive semicircles in the high and low frequency sides of the spectrum for all alcohols. The depressed semicircle in the high frequency region might be related to the combination of charge transfer resistance and the double layer capacitance. The low frequency semicircle was attributed to the adsorption of the reaction intermediate on the electrode surface. Bode phase plots for the same sample are shown in Figure 5(b). Two distinguishable peaks are observed in the Bode plots corresponding to two depressed semicircles in the Nyquist plot.

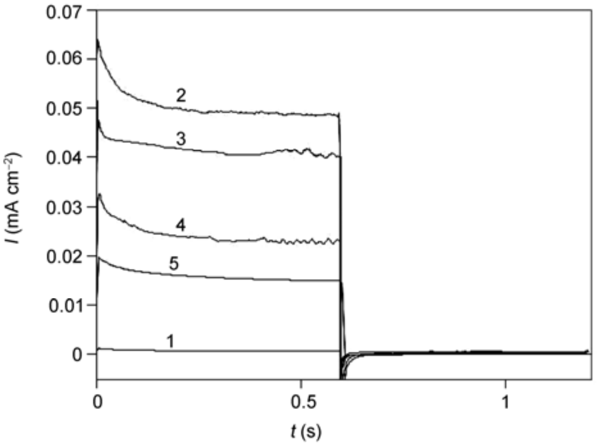

Figure 3 Double steps chronoamperograms of G/Ni electrode in 1 M NaOH solution in the absence (1) and presence of 0.1 M of (2) methanol, (3) ethanol, (4) 1-propanol and (5) 2-propanol. Potential steps were 650 and 300 mV, respectively.

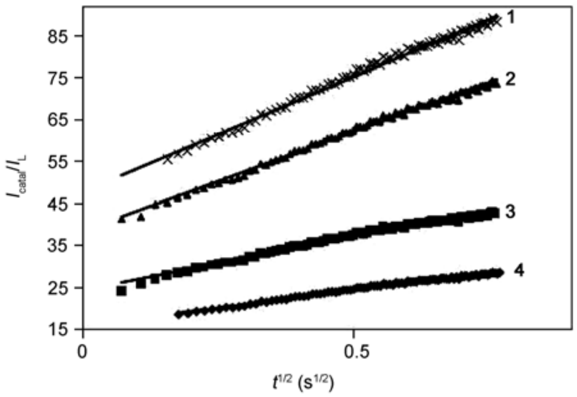

Figure 4 Dependence of $I_{\text{cat}}/I_{\text{L}}$ on $t^{1/2}$ derived from the data of chronoamperograms of (1) methanol, (2) ethanol, (3) 1-propanol and (4) 2-propanol from Figure 3.

The equivalent circuit compatible with the Nyquist diagram recorded in the presence of alcohols is depicted in Figure 6. To obtain a satisfactory impedance simulation of alcohols electro-oxidation, it is necessary to replace the capacitor C with a constant phase element (CPE), Q, in the equivalent circuit. The most widely accepted explanation for the presence of CPE behavior and depressed semicircles on solid electrodes is microscopic roughness, causing an

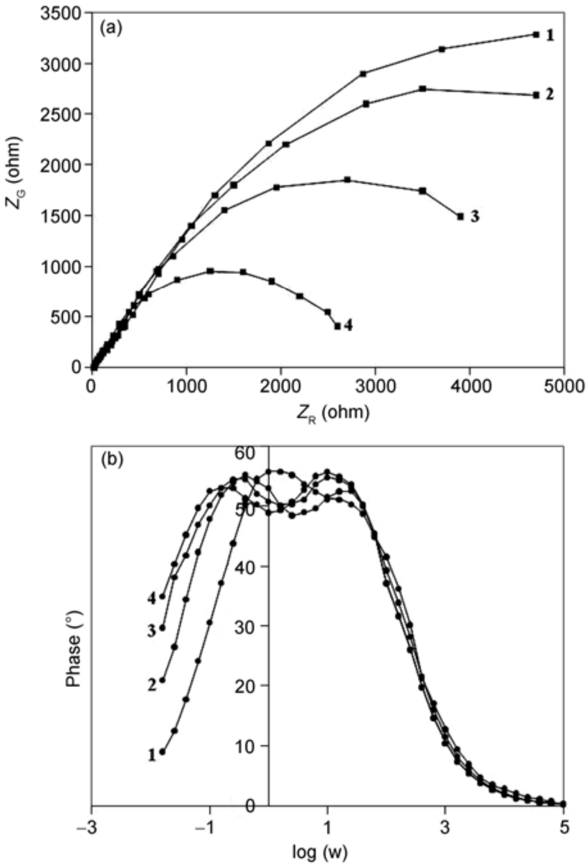

Figure 5 (a) Nyquist diagrams; (b) phase shift plot of the G/Ni electrode for (1) 2-propanol, (2) 1-propanol, (3) ethanol and (4) methanol in 1 M NaOH. DC potential is 650 mV vs. Ag/AgCl.

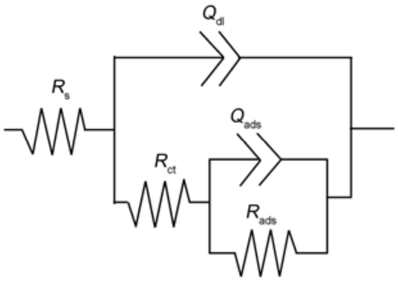

Figure 6 Equivalent circuits compatible with the Nyquist diagrams in Figure 5 for low carbon alcohols electrooxidation on the G/Ni electrode.

Table 1 Equivalent circuit parameters of electrooxidation of alcohols on the G/Ni electrode in NaOH solution obtained from Figure 5

Alcohol	R_s (Ω)	R_{ct} (Ω)	$Q_{dl}\times10^3$ (F)	$R_{ads}\times10^{-3}$ (Ω)	$Q_{ads}\times10^3$ (F)	n_1	n_2
Methanol	15.5	251	1.05	2.45	1.08	0.81	0.8
Ethanol	15.8	420	1.02	4.82	1.6	0.85	0.75
1-Propanol	15.7	615	1.1	7.2	1.8	0.8	0.78
2-propanol	15.5	730	1.1	8.65	1.95	0.82	0.82

inhomogeneous distribution in the solution resistance as well as in the double-layer capacitance [40]. In this electrically equivalent circuit, R_s, CPE$_{dl}$ and R_{ct} represent solution resistance, a constant phase element corresponding to the double layer capacitance and the charge transfer resistance. CPE$_{ads}$ and R_{ads} are the electrical elements related to the adsorption of reaction intermediates. In this circuit, the charge transfer resistance of the electrode reaction has a simple physical meaning indicating how fast charge transfer occurs during alcohol electrooxidation at the surface of the electrode.

To corroborate the equivalent circuit, the experimental data are fitted to equivalent circuit and the circuit elements are obtained. Table 1 illustrates the equivalent circuit parameters for the impedance spectra of alcohols oxidation at different number of carbon. As shown in Table 1, with increasing the number of carbon, the diameters of both semicircles are increased.

4 Conclusion

The nickel oxide film was formed electrochemically on electrodeposited nickel in a regime of cyclic voltammetry on a graphite electrode and tested for electro-oxidation of alcohols in alkaline media. The modified electrodes showed electrocatalytic activity for the oxidation of low carbon alcohols, while the graphite electrode presents no activity. In CV studies, in the presence of alcohols Ni modified electrode shows an activity order of methanol > ethanol > 1-propanol > 2-propanol. Double steps chronoamperograms for the G/Ni in the presence of alcohols show an irreversible process and higher catalytic rate constant obtained for methanol oxidation rather than higher carbon alcohols. Charge transfer resistance was obtained for different low carbon oxidation and indicated that methanol oxidation on G/Ni electrode progressed with higher exchange current density.

1 Danaee I, Jafarian M, Gobal F, Sharafi M, Mahjani MG. Electrochemical impedance of ethanol oxidation in alkaline eedia. *Chem Res Chinese Universities*, 2012, 28: 19-25

2 Vigier F, Coutanceau C, Hahn F, Belgsir EM, Lamy C. On the mechanism of ethanol electro-oxidation on Pt and PtSn catalysts: Electrochemical and in situ IR reflectance spectroscopy studies. *J Electroanal Chem*, 2004, 563: 81-89

3 Secanell M, Wishart J, Dobson P. Computational design and optimization of fuel cells and fuel cell systems: A review. *J Power sources*, 2011, 196: 3690-3704

4 Feng L, Zhang J, Cai W, Liang L, Xing W, Liu C. Single passive direct methanol fuel cell supplied with pure methanol. *J Power sources*, 2011, 196: 2750-2753

5 Danaee I, Jafarian M, Mirzapoor A, Gobal F, Mahjani MG. Electrooxidation of methanol on NiMn alloy modified graphite electrode. *Electrochim Acta*, 2010, 55: 2093-2100

6 Feng L, Zhao X, Yang J, Xing W, Liu C. Electrocatalytic activity of Pt/C catalysts for methanol electrooxidation promoted by molybdovanadophosphoric acid. *Catal Commun*, 2011, 14: 10-14

7 Lamy C, Lima A, LeRhun V, Delime F, Coutanceau C, Léger JM. Recent advances in the development of direct alcohol fuel cells (DAFC). *J Power sources*, 2002, 105:283-296

8 Rodrigues LDA, De Souza JPI, Pastor E, Nart FC. Cleavage of the C–C bond during the electrooxidation of 1-propanol and 2-propanol: Effect of the Pt morphology and of codeposited Ru. *Langmuir*, 1997, 13: 6829-6835

9 Sun SG, Lin Y. *In situ* FTIR spectroscopic investigations of reaction mechanism of isopropanol oxidation on platinum single crystal electrodes. *Electrochim Acta*, 1996, 41: 693-700

10 Fujiwara N, Siroma Z, Ioroi T, Yasuda K. Rapid evaluation of the electrooxidation of fuel compounds with a multiple-electrode setup for direct polymer electrolyte fuel cells. *J Power Sources*, 2007, 164: 457-463

11 Liu J, Ye J, Xu C, Jiang SP, Tong Y. Electro-oxidation of methanol, 1-propanol and 2-propanol on Pt and Pd in alkaline medium. *J Power Sources*, 2008, 177: 67-70

12 Santasalo A, Vidal-Iglesias FJ, Solla-Gullón J, Berná A, Kallio T, Feliu JM. Electrooxidation of methanol and 2-propanol mixtures at platinum single crystal electrodes. *Electrochim Acta*, 2009, 54: 6576-6583

13 Cheng Y, Liu Y, Cao D, Wang G, Gao Y. Effects of acetone on electrooxidation of 2-propanol in alkaline medium on the Pd/Ni-foam electrode. *J Power Sources*, 2011, 196: 3124-3128

14 Danaee I, Jafarian M, Forouzandeh F, Gobal F, Mahjani MG. Electrocatalytic oxidation of methanol on Ni and NiCu alloy modified glassy carbon electrode. *Int J Hydrogen Energy*, 2008, 33: 4367-4376

15 Antolini E. Catalysts for direct ethanol fuel cells. *J Power sources*, 2007, 170: 1-12

16 Danaee I, Jafarian M, Forouzandeh F, Gobal F, Mahjani MG. Electrochemical impedance studies of methanol oxidation on GC/Ni and GC/NiCu electrode. *Int J Hydrogen Energy* 2009, 34: 859-869

17 Tian T, Liu C, Liao J, Xing W, Lu T. The enhancement effect of Eu^{3+} on electro-oxidation of ethanol at Pt electrode. *J Power sources*, 2007, 174: 176-179

18 Antolini E. Formation of carbon-supported PtM alloys for low temperature fuel cells: A review. *Mater Chem Phys* 2003, 78: 563–573

19 King WD, Corn JD, Murphy OJ, Boxall DL, Kenik EA, Kwiatkowski KC. Pt–Ru and Pt–Ru–P/carbon nanocomposites: Synthesis, characterization, and unexpected performance as direct methanol fuel cell (DMFC) anode catalysts. *J Phys Chem*, 2003,107: 5467–5474

20 Park IS, Park KW, Choi JH, Park CR, Sung YE. Electrocatalytic enhancement of methanol oxidation by graphite nanofibers with a high loading of PtRu alloy nanoparticles. *Carbon*, 2007, 45: 28-33

21 Feng L, Yan L, Cui Z, Liu C, Xing W. High activity of Pd–WO$_3$/C catalyst as anodic catalyst for direct formic acid fuel cell. *J Power sources*, 2011, 196: 2469-2474

22 Cui Z, Feng L, Liu C, Xing W. Pt nanoparticles supported on WO_3/C hybrid materials and their electrocatalytic activity for methanol electro-oxidation. *J Power sources*, 2011, 196: 2621-2626

23 Wen TC, Lin SM, Tsai JM. Sulphur content and the hydrogen evolving activity of NiS*x* deposits using statistical experimental strategies. *J Appl Electrochem*, 1994, 24: 233-238

24 Fan C, Piron DL, Sleb A, Paradis P. Study of electrodeposited nickel-molybdenum, nickel-tungsten, cobalt–molybdenum, and cobalt-tungsten as hydrogen electrodes in alkaline water electrolysis. *J Electrochem Soc*, 1994, 141: 382-387

25 Raj LA, Vasu KI. Transition metal-based hydrogen electrodes in alkaline solution—electrocatalysis on nickel based binary alloy coatings. *J Appl Electrochem*, 1991, 32: 32-38

26 Casadei MA, Pletcher D. The influence of conditions on the electrocatalytic hydrogenation of organic molecules. *Electrochim Acta*, 1988, 33: 117-1120

27 Berchmans S, Gomathi H, Prabhakara Rao G. Electrooxidation of alcohols and sugars catalysed on a nickel oxide modified glassy carbon electrode. *J Electroanal Chem*, 1995, 394: 267-270

28 Fleischmann M, Korinek K, Pletcher D. The kinetics and mechanism of the oxidation of amines and alcohols at oxidecovered nickel, silver, copper, and cobalt electrodes. *J Chem Soc Perkin Trans*, 1972, 2: 1396-1402

29 Taraszewska J, Roslonek G. Electrocatalytic oxidation of methanol on a glassy carbon electrode modified by nickel hydroxide formed by ex situ chemical precipitation. *J Electroanal Chem*, 1994, 364: 209-213

30 Danaee I. Kinetics and mechanism of palladium electrodepositon on graphite electrode by impedance and noise measurements. *J Electroanal Chem*, 2011, 662: 415-420

31 El-Shafei AA. Electrocatalytic oxidation of methanol at a nickel hydroxide/glassy carbon modified electrode in alkaline medium. *J Electroanal Chem*, 1999, 471: 89-95

32 Jafarian M, Forouzandeh F, Danaee I, Gobal F, Mahjani MG. Electrocatalytic oxidation of glucose on Ni and NiCu alloy modified glassy carbon electrode. *J Solid State Electrochem*, 2009, 13: 1171-1179

33 Hahn F, Beden B, Croissant MG, Lamy C. *In situ* UV visible reflectance spectroscopic investigation of the nickel electrodealkaline solution interface. *Electrochim Acta*, 1986, 31: 335-342

34 Desilvestro J, Corrigan DA, Weaver MJ. Characterization of redox states of nickel hydroxide filmelectrodes by *in situ* surface Raman spectroscopy. *J Electrochem Soc*, 1988, 135: 885-892

35 Barnard R, Randell CF. Studies concerning charged nickel hydroxide electrodes. VII. Influence of alkali concentration on anodic peak positions. *J Appl Electrochem*, 1983, 13: 89-95

36 Fleischmann M, Korinek MK, Pletcher D. The oxidation of organic compounds at a nickel anode in alkaline solution. *J Electroanal Chem*, 1971, 31: 39-49

37 Danaee I, Jafarian M, Forouzandeh F, Gobal F, Mahjani MG. Kinetic interpretation of a negative time constant impedance of glucose electrooxidation. *J Phys Chem B*, 2008, 112: 15933-15940

38 Danaee I, Jafarian M, Forouzandeh F, Gobal F, Mahjani MG. Impedance spectroscopy analysis of glucose electro-oxidation on Ni-modified glassy carbon electrode. *Electrochim Acta*, 2008, 53: 6602-6609

39 Bard AJ, Faulkner LR. *Electrochemical Methods*. New York: Wiley, 2001

40 Danaee I, Noori S. Kinetics of the hydrogen evolution reaction on NiMn graphite modified electrode. *Int J Hydrogen Energy*, 2011, 36: 12102-12111